

STUDIES ON SYNTHESIS AND CHARACTERIZATION OF NANOCARBON FROM RICE HUSK CHAR

Zaw Oo¹, Yi Yi Myint²

Abstract

In this research work, some physicochemical properties of rice husk raw and rice husk char were determined by AOAC method. The nanocarbons were prepared from rice husk char with NaNO_3 , KMnO_4 and H_2SO_4 by modified Hummer Method under different conditions. Similarly, nanocarbons were prepared from rice husk char with H_3PO_4 , KMnO_4 and H_2SO_4 by the same method under different conditions. The synthesized nanocarbons were also characterized by using X-ray diffraction analysis (XRD) and Scanning Electron Microscopy analysis (SEM) techniques.

Keywords: physicochemical, Nanocarbon, Hummer method, XRD, SEM

Introduction

A carbon-based material whose constituents are of nanoscale dimensions, or which is produced by nanotechnology. Nanomaterials are currently on the cutting edge of material science research and are gradually finding applications in our daily life, including life science, energy, and environmental applications. Among many nanomaterials, carbon nanomaterials such as carbon nanotubes (CNTs), graphite, diamonds, fullerenes, and graphene, with their high specific surface areas and large pore volumes, have remained at the forefront of nanotechnology. In this study nanocarbons were synthesized from rice husk biochar (Figure 1).

(a) Rice husk

Rice husk are the hard protecting coverings of grains of rice and part of the chaff of the rice. Rice hulls are the coatings of seeds, or grains, of rice. The husk protects the seed during the growing season, since it is formed from hard materials, including opaline silica and lignin. Rice husk is used as building material, fertilizer, insulation material and fuel.

(b) Rice husk biochar

Biochar is a type of black carbon produced from a carbonaceous material through the application of heat or chemicals. Biochar is a carbon rich highly porous substance obtained after pyrolysis of organic biomass. Production of biochar is a sustainable option for waste and disease management. It contains 50 % of the original carbon which is highly recalcitrant in nature; therefore its production helps in carbon sequestration by locking the carbon present in the plant biomass. Biochar is used as a tool for waste management, as a soil conditioner, treatment of waste water, building sector, cosmetic industries, metallurgy, food industry and energy production.

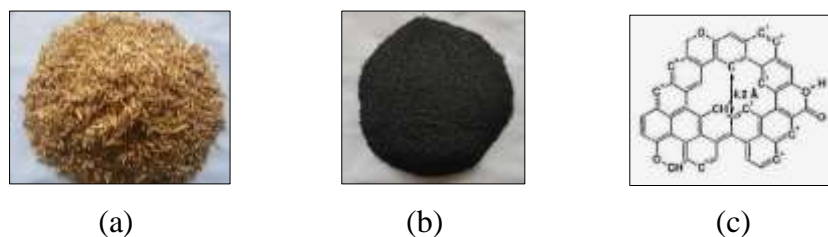


Figure 1 (a) Rice husk (b) Rice husk biochar and (c) Composition of biochar

¹ 3PhD Candidate, Department of Chemistry, Mandalay University

² Dr, Professor and Head, Department of Chemistry, University of Mandalay

(c) Nanocarbons

(i) Fullerenes

Fullerene is a spherical carbon compound and is an allotrope of carbon such as diamond, graphite and carbon nanotubes. Fullerenes of C₆₀, C₇₀ and C₈₄ are well known. They are isolable carbon compounds in a sole molecular species. Among them, the C₆₀ is a representative species. Kroto, Smalley and Curl first observed the C₆₀ in which the 60 carbon atoms consist of 12 five-membered rings and 20 six-membered rings and won their joint Nobel prizes in chemistry in 1996 for their contributions (Kroto *et al.*, 1985). Osawa predicted existence of fullerene in 1970, earlier than the first observation of fullerene.

(ii) Carbon nanotubes

A carbon nanotube (CNT) has a cylindrical structure with a nanoscale diameter that is like a rolled graphene sheet. Iijima first observed a CNT in 1991. A CNT consists of only sp² carbons similar to fullerenes. There are diverse CNTs on the basis of their length, diameter of the nanotube, state of chirality, and number of the layer. The variety of these structures provides various band structures and metallic and semiconducting properties. A normal synthetic procedure gives a mixture of semiconducting CNTs in 2/3 and metallic CNTs in 1/3, because rolling a carbon sheet occurs randomly.

(iii) Graphene/graphene oxides

Graphene, which is one of the nanocarbon materials, consists of all six-membered rings with sp² carbons having a twodimensional sheet structure. Graphene has been known for long time, since graphite is formed by combination of graphenes with van der Waals force. However, details of the properties were unclear until late years, because an isolation procedure of graphene from graphite was not well developed for long time. Geim and Novoselov *et al.* in 2004 successfully isolated a thinflake graphene by a simple procedure. They used a tape to peel off a graphene layer from highly oriented pyrolytic graphite (HOPG) and then the peeled graphene layer is stuck on a substrate. After this observation, studies of graphene have proved the particular characteristics of electronic, mechanical, and chemical properties. Geim and Novoselov won their joint Nobel prizes in physics in 2010 for their contributions (Geim, 2009; Novoselov, 2005).

(iv) Nanodiamonds

Diamond, an allotrope of carbon, has excellent hardness, coefficient of friction, thermal conductivity, insulation characteristics, and refractive index. Large and highly pure diamond is good for use as jewelry. Furthermore, the major industrial application of diamond is for cutting and polishing tools, because it is the hardest of natural products. However, diamond is not workable enough because of its hardness so there is a limitation for industrial use of a large diamond. Nanodiamond (ND) is a nanoparticle having the crystal structure of diamond, and it has excellent properties of normal diamond. ND is artificially synthesized for additives of engine oil.

(v) Nanocarbon unit structures

Cycloparaphenylenes (CPP)

Carbon nanotubes (CNT) have advanced chemistry, material science, life science and other research fields. CNTs can be prepared by physical methods such as arc discharge, laser furnace, and chemical vapor deposition techniques. One disadvantage of these physical methods is forming several kinds of CNTs with various diameters, thus uniform CNTs do not form. Cycloparaphenylenes (CPP), the so-called carbon nanoring, have a cyclic structure formed by

linkages of *p*-substituted benzenes. The CPP attracted researchers in fundamental chemistry and material science, because it is a unit structure of CNT.

(d) Characterization of nanoparticle

1. XRD measurement

X-ray diffraction analysis of nanoparticle was conducted using X-ray diffractometer equipment with a Cu K α radiation at an accelerating voltage 40 kV and emission current 30 mA in the range of diffraction angle $2\theta = 10 - 80^\circ$. The XRD analysis was conducted to investigate the interlayer spacing of the prepared sample.

2. SEM measurement

The Scanning Electron Microscopy analysis was conducted to study the changes in surface morphology such as smoothness and roughness of sample. Samples were coated with gold prior to recording of images for rendering the same conductivity.

3. Debye-Scherrer's Equation

The average particles of prepared powders were calculated by "Debye-Scheerer Equation" using XRD line broadening method.

$$D = \frac{K\lambda}{\beta \cos \theta}$$

Where, D = the mean size of crystallites (nm)

K= crystallite shape factor

λ = the wavelength of incident X-ray

β = full width at high maximum in radians of the X-ray diffraction peak

θ = Bragg's angle

4. Bragg's Law Equation

The interplanar spacing in nm of prepared powders was calculated by "Bragg's Law Equation" using XRD line broadening method.

$$n\lambda = 2d \sin \theta$$

Where, d = interplanar spacing nm

Materials and Methods

Sampling

The rice husk raw was collected from Nabekan Village, Wundwin Township, Mandalay Region (Figure 2). The sample was first cleaned and washed with water. And then, the collected samples were kept in air to dry at room temperature for a few weeks. Biochar was prepared from rice husk by AOAC method (A.O.A.C, 2000).

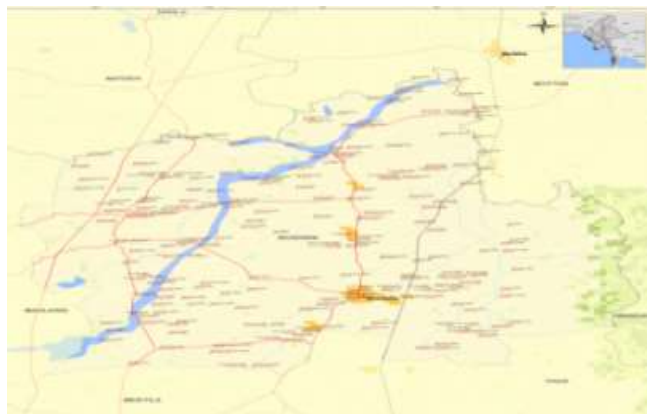


Figure 2 Nabekan Village, Wundwin Township, Mandalay Region.

Some physicochemical properties of rice husk raw and rice husk char such as ash content, pH values and moisture content were determined by the A.O.A.C method (A.O.A.C, 2000).

Preparation of nanocarbons NC-1 from rice husk char with NaNO₃, KMnO₄ and H₂SO₄ (6 h stirring time)

Procedure

0.5 g of rice husk char was mixed with 0.25 g of sodium nitrate and was stirred in ice bath. After that, 20 mL of concentrated sulphuric acid was added (drop by drop along to the wall of the beaker) to the above mixture and then, 2 g of potassium permanganate was slowly added and was stirred in ice bath for 1 h. Then, the whole mixture was stirred at room temperature for 3 h. After that, 50 mL of water was added to the mixture and stirred for 1 h. Then, 50 mL of hot water and 7.5 mL of 30 % H₂O₂ solution were added drop by drop to the mixture and it was stirred for 1 h. Finally, the mixture was filtered and the filtered powder by washing with 5 % HCl solution and washed with distilled water till neutral to get NC-1 powder.

Similarly, NC-2(stirring time 8 h), NC-3(using double amount of NaNO₃, KMnO₄ and H₂SO₄), NC-4(stirring time 3 h and sonication time 3 h), NC-5(stirring time 3.5 h and sonication time 4.5 h), NC-6(using double amount of NaNO₃, KMnO₄ and H₂SO₄, stirring time 3 h and sonication time 3 h) were prepared using the same procedure as described for NC-1.

Preparation of nanocarbon NC-7 from rice husk char with H₃PO₄, KMnO₄ and H₂SO₄ (6.5 h stirring time)

Procedure

0.5 g of rice husk char was mixed with 3mL of phosphoric acid and was stirred in ice bath. After that, 27 mL of concentrated sulphuric acid was added (drop by drop along to the wall of the beaker) to the above mixture and then, 1.32 g of potassium permanganate was slowly added and was stirred in ice bath for 1.5 h. Then, the whole mixture was stirred for 4.5 h. After that, 1 mL of concentrated H₂O₂ solution was added drop by drop to the mixture and was stirred for 0.5 h. Then 10 mL of concentrated HCl was added drop by drop and 30 mL of water was added to the mixture. Finally, the mixture was filtered and the filtered powder was washed with distilled water till neutral to get NC-7 powder.

Similarly, NC-8(stirring time 10 h), NC-9(using double amount of phosphoric acid, KMnO₄ and H₂SO₄) and NC-10(stirring time 3 h and sonication time 7 h) were prepared using the same procedure as described for NC-7.

Characterization of synthesized nanocarbons from rice husk char

XRD analysis

Powder X-ray diffraction (XRD) patterns were performed using a RIGAKU Multiplex 2k W, X-ray diffractometer with Cu K α radiation of wavelength 1.54056 Å

SEM Analysis

The samples were examined by Scanning Electron Microscope (SEM) for a visual inspection of external porosity, and morphology.

Results and Discussion

Determination of ash content, pH values and moisture content

The ash content, pH values and moisture content of rice husk raw and rice husk charcoal were determined by AOAC method. The results are shown in Table 1.

Table 1 Determination of ash content, pH values, and moisture content of rice husk raw and rice husk char

No	Properties	Rice husk raw	Rice husk char	Apparatus used
1	Ash (%)	16.14	32.59	Muffle furnace
2	pH	7.82	7.84	pH meter
3	Moisture (%)	8.76	4.09	Oven

From the results, the pH values of the two samples are nearly the same, but the ash content of rice husk charcoal is twice of the ash content of rice husk raw and the moisture content of rice husk charcoal is half of the moisture content of rice husk raw. Among these two samples, rice husk char was selected for the study.

XRD Analysis of Synthesized Nanocarbon NC-1 from Rice Husk Char

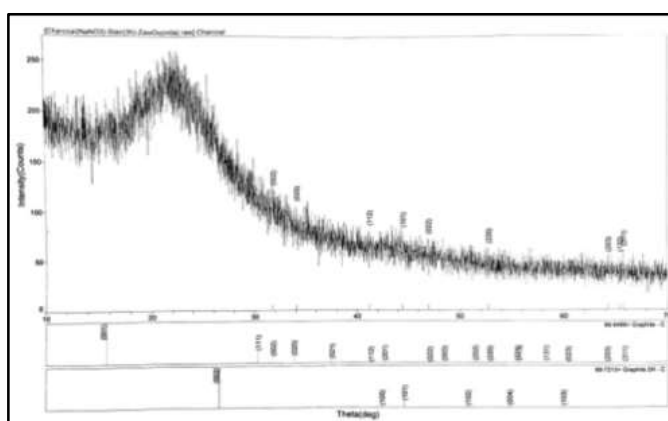


Figure 3 XRD diffraction pattern of nanocarbon NC-1 from rice husk char

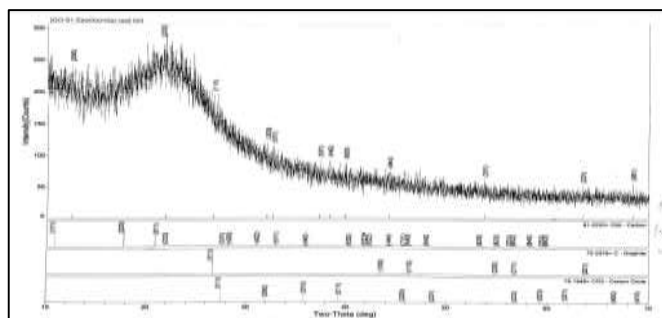
The crystallite size and crystal structure of nanocarbon NC-1 from the rice husk char was determined from the XRD study.

Table 2 The average particle size of nanocarbon NC-1 from rice husk char

Peak No.	Bragg angle (2θ)	Miller indices (h k l)	FWHM of peak (β) radians	Particle size, D (nm)
1	31.741	(0 0 2)	0.0083	17.174
2	34.024	(0 2 0)	0.0027	53.105
3	41.183	(1 1 2)	0.0014	104.620
4	44.464	(1 0 1)	0.0063	23.511
5	46.953	(0 2 2)	0.0023	64.993
6	52.752	(2 2 0)	0.0046	33.270

The localized peaks at $2\theta = 31.741^\circ$, 34.024° , 41.183° , 44.464° , 46.953° and 52.752° that referred to plane reflections of (002), (020), (112), (101), (022) and (220), respectively. According to Table 5, the range of particle size of synthesized nanocarbon NC-1 from rice husk char was found to be 17.174nm-104.620 nm and average particle size is 44.232 nm.

XRD Analysis of Synthesized Nanocarbon NC-2 from Rice Husk Char

**Figure 4** XRD diffraction pattern of nanocarbon NC-2 from rice husk char

The crystallite size and crystal structure of nanocarbon NC-2 from the rice husk char was determined from the XRD study.

Table 3 The average particle size of nanocarbon NC-2 from rice husk char

Peak No.	Bragg angle (2θ)	Miller indices (h k l)	FWHM of peak (β) radians	Particle size, D (nm)
1	12.497	(2 0 0)	0.0094	14.673
2	21.792	(2 2 2)	0.0039	35.802
3	26.604	(1 1 1)	0.0044	32.020
4	53.930	(3 1 1)	0.0027	56.976
5	63.568	(2 2 1)	0.0071	22.718
6	68.460	(9 5 1)	0.0027	61.420

The localized peaks at $2\theta = 12.497^\circ$, 21.792° , 26.604° , 53.930° , 63.568° and 68.460° that referred to plane reflections of (200), (222), (111), (311), (221) and (951), respectively. The broad peak at around 26° confirms the presence of amorphous nanocarbon material. According to Table 3, the range of particle size of synthesized nanocarbon NC-2 from rice husk char was found to be 14.673nm-61.420 nm and average particle size is 32.5489 nm.

XRD Analysis of Synthesized Nanocarbon NC-3 from Rice Husk Char

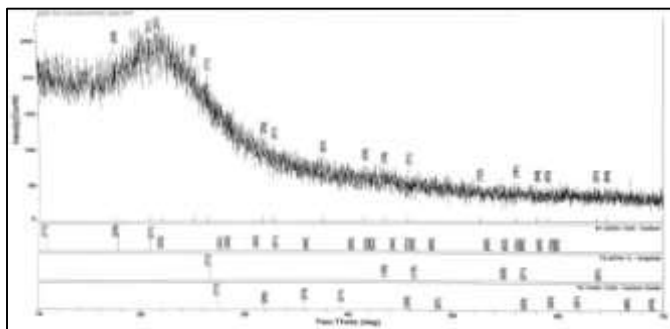


Figure 5 XRD diffraction pattern of nanocarbon NC-3 from rice husk char

The crystallite size and crystal structure of nanocarbon NC-3 from the rice husk char was determined from the XRD study.

Table 4 The average particle size of nanocarbon NC-3 from rice husk char

Peak No.	Bragg angle (2θ)	Miller indices (h k l)	FWHM of peak (β) radians	Particle size, D (nm)
1	17.438	(2 2 0)	0.0047	29.513
2	20.840	(3 1 1)	0.0062	22.485
3	21.901	(2 2 2)	0.0092	15.180
4	43.511	(1 0 0)	0.0095	15.539
5	45.935	(7 1 1)	0.0027	50.850
6	56.143	(7 5 1)	0.0017	91.406

The localized peaks at $2\theta = 17.438^\circ, 20.840^\circ, 21.901^\circ, 43.511^\circ, 45.935^\circ$ and 56.143° that referred to plane reflections of (220), (311), (222), (100), (711) and (751), respectively. The broad peak at around 26° confirms the presence of amorphous nanocarbon material. According to Table 4, the range of particle size of synthesized nanocarbon NC-3 from rice husk char was found to be 15.180nm-91.406 nm and average particle size is 34.7114 nm.

XRD Analysis of Synthesized Nanocarbon NC-4 from Rice Husk Char

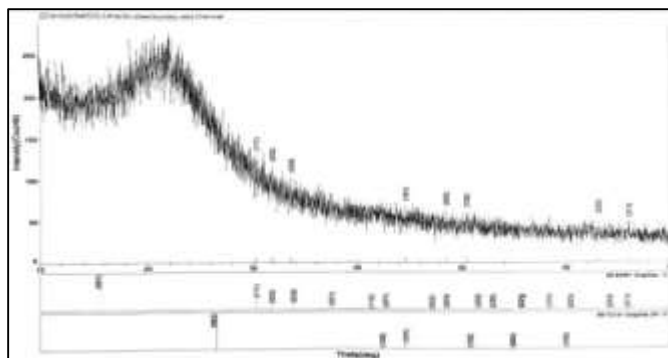


Figure 6 XRD diffraction pattern of nanocarbon NC-4 from rice husk char

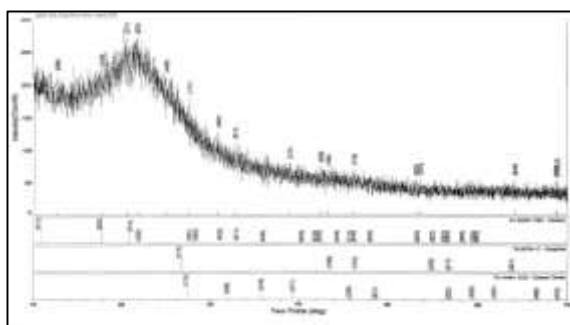
The crystallite size and crystal structure of nanocarbon NC-4 from the rice husk char was determined from the XRD study.

Table 5 The average particle size of nanocarbon NC-4 from rice husk char

Peak No.	Bragg angle (2 θ)	Miller indices (h k l)	FWHM of peak (β) radians	Particle size, D (nm)
1	30.247	(1 1 1)	0.0016	88.768
2	31.776	(0 0 2)	0.0040	35.639
3	33.582	(0 2 0)	0.0063	22.733
4	44.615	(1 0 1)	0.0027	54.889
5	48.509	(0 0 3)	0.0075	20.051
6	63.101	(2 2 2)	0.0018	89.385

The localized peaks at $2\theta = 30.247^\circ$, 31.776° , 33.582° , 44.615° , 48.509° and 63.101° that referred to plane reflections of (111), (002), (020), (101), (003) and (222), respectively. According to Table 5, the range of particle size of synthesized nanocarbon NC-4 from rice husk char was found to be 20.051nm-89.385nm and average particle size is 47.163 nm.

XRD Analysis of Synthesized Nanocarbon NC-5 from Rice Husk Char

**Figure 7** XRD diffraction pattern of nanocarbon NC-5 from rice

The crystallite size and crystal structure of husk char nanocarbon NC-5 from the rice husk char was determined from the XRD study.

Table 6 The average particle size of nanocarbon NC-5 from rice husk char

Peak No.	Bragg angle (2 θ)	Miller indices (h k l)	FWHM of peak (β) radians	Particle size, D (nm)
1	12.684	(2 0 0)	0.0063	21.898
2	17.666	(2 2 0)	0.0049	28.317
3	20.531	(3 1 1)	0.0050	27.868
4	21.717	(2 2 2)	0.0072	19.390
5	24.911	(4 0 0)	0.0050	28.083
6	27.462	(1 1 1)	0.0014	100.816
7	64.179	(8 4 4)	0.0015	107.890

The localized peaks at $2\theta = 12.684^\circ$, 17.666° , 20.531° , 21.717° , 24.911° , 27.462° and 64.179° that referred to plane reflections of (200), (220), (311), (222), (400), (111) and (844), respectively. The broad peak at around 26° confirms the presence of amorphous nanocarbon material. According to Table 6, the range of particle size of synthesized nanocarbon NC-5 from rice husk char was found to be 19.390nm-107.890 nm and average particle size is 42.2241 nm.

XRD Analysis of Synthesized Nanocarbon NC-6 from Rice Husk Char

The crystallite size and crystal structure of nanocarbon NC-6 from the rice husk char was determined from the XRD study.

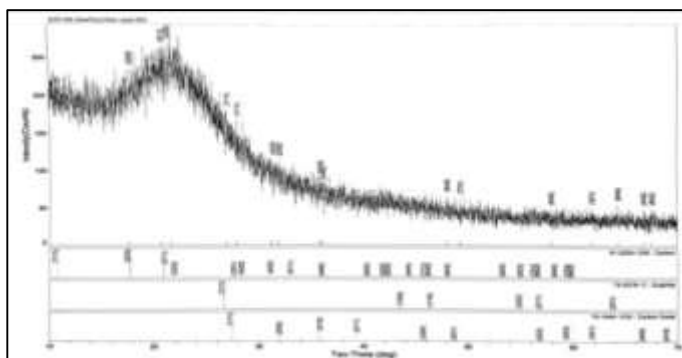


Figure 8 XRD diffraction pattern of nanocarbon NC-6 from rice husk char

Table 7 The average particle size of nanocarbon NC-6 from rice husk char

Peak No.	Bragg angle (2θ)	Miller indices (h k l)	FWHM of peak (β) radians	Particle size, D (nm)
1	17.579	(2 2 0)	0.0064	21.678
2	20.587	(3 1 1)	0.0059	23.619
3	21.521	(2 2 2)	0.0072	19.384
4	26.733	(1 1 1)	0.0048	29.360
5	27.710	(1 1 1)	0.0029	48.696
6	67.582	(8 6 2)	0.0024	68.724

The localized peaks at $2\theta = 17.579^\circ, 20.587^\circ, 21.521^\circ, 26.733^\circ, 27.710^\circ$ and 67.582° that referred to plane reflections of (220), (311), (222), (111), (111) and (862), respectively. The broad peak at around 26° confirms the presence of amorphous nanocarbon material. According to Table 7, the range of particle size of synthesized nanocarbon NC-6 from rice husk char was found to be 19.384nm-68.742 nm and average particle size is 35.2175 nm.

XRD Analysis of Synthesized Nanocarbon NC-7 from Rice Husk Char

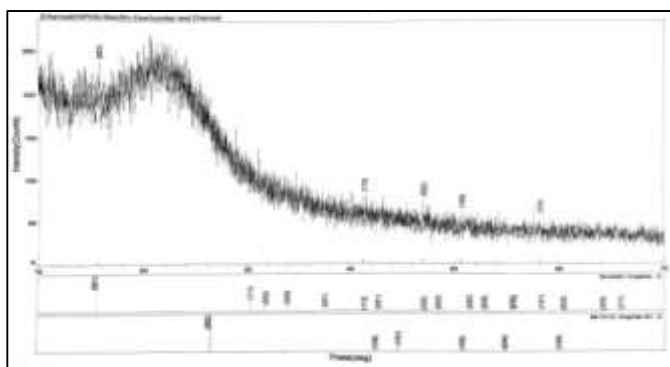


Figure 9 XRD diffraction pattern of nanocarbon NC-7 from rice husk char

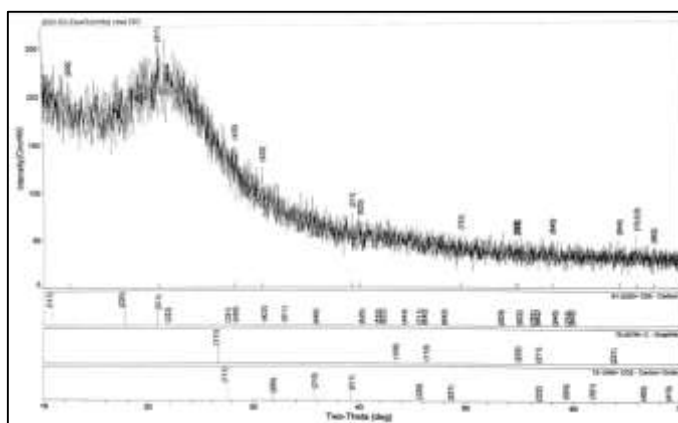
The crystallite size and crystal structure of nanocarbon NC-7 from the rice husk char was determined from the XRD study.

Table 8 The average particle size of nanocarbon NC-7 from rice husk char

Peak No.	Bragg angle (2θ)	Miller indices (h k l)	FWHM of peak (β) radians	Particle size, D (nm)
1	15.697	(0 0 1)	0.0054	25.630
2	41.226	(1 1 2)	0.0053	27.639
3	46.990	(0 2 2)	0.0046	32.501
4	50.693	(1 0 2)	0.0047	32.280
5	58.155	(1 3 1)	0.0038	41.285

The localized peaks at $2\theta = 15.697^\circ$, 41.226° , 46.990° , 50.693° and 58.155° that referred to plane reflections of (001), (112), (022), (102) and (131), respectively. According to Table 8, the range of particle size of synthesized nanocarbon NC-7 from rice husk char was found to be 25.630nm-41.285 nm and average particle size is 31.867 nm.

XRD Analysis of Synthesized Nanocarbon NC-8 from Rice Husk Char

**Figure 10** XRD diffraction pattern of nanocarbon NC-8 from rice husk char

The crystallite size and crystal structure of nanocarbon NC-8 from the rice husk char was determined from the XRD study.

Table 9 The average particle size of nanocarbon NC-8 from rice husk char

Peak No.	Bragg angle (2θ)	Miller indices (h k l)	FWHM of peak (β) radians	Particle size, D (nm)
1	12.482	(2 0 0)	0.0080	17.241
2	20.908	(3 1 1)	0.0056	24.897
3	28.089	(4 2 0)	0.0055	25.697
4	30.738	(4 2 2)	0.0029	49.033
5	39.339	(2 1 1)	0.0052	28.006
6	54.783	(2 2 2)	0.0027	57.194

The localized peaks at $2\theta = 12.482^\circ$, 20.908° , 28.089° , 30.738° , 39.339° and 54.783° that referred to plane reflections of (200), (311), (420), (422), (211) and (222), respectively. The broad peak at around 26° confirms the presence of amorphous nanocarbon material. According to Table 9, the range of particle size of synthesized nanocarbon NC-8 from rice husk char was found to be 17.241nm-57.194 nm and average particle size is 36.8098 nm.

XRD Analysis of Synthesized Nanocarbon NC-9 from Rice Husk Char

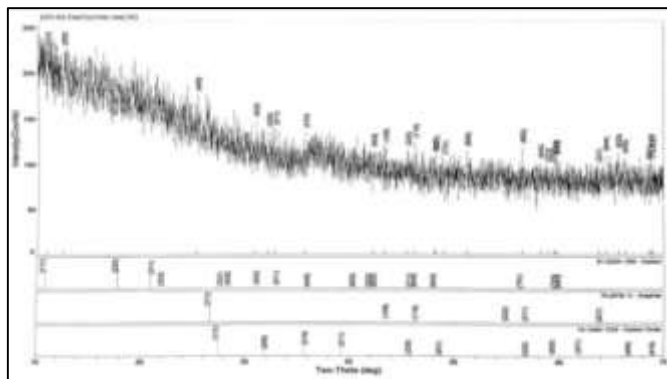


Figure 11 XRD diffraction pattern of nanocarbon NC-9 from rice husk char

The crystallite size and crystal structure of nanocarbon NC-9 from the rice husk char was determined from the XRD study.

Table 10 The average particle size of nanocarbon NC-9 from rice husk char

Peak No.	Bragg angle (2θ)	Miller indices (h k l)	FWHM of peak (β) radians	Particle size, D (nm)
1	10.887	(1 1 1)	0.0049	28.108
2	12.489	(2 0 0)	0.0042	32.840
3	25.191	(4 0 0)	0.0020	70.246
4	58.944	(0 2 3)	0.0134	11.753
5	59.480	(7 5 3)	0.0080	19.739
6	59.643	(7 5 3)	0.0010	158.037

The localized peaks at $2\theta = 10.887^\circ, 12.489^\circ, 25.191^\circ, 58.944^\circ, 59.480^\circ$ and 59.643° that referred to plane reflections of (111), (200), (400), (023), (753) and (753), respectively. The broad peak at around 26° confirms the presence of amorphous nanocarbon material. According to Table 10, the range of particle size of synthesized nanocarbon NC-9 from rice husk char was found to be 11.753nm-158.037 nm and average particle size is 44.1708 nm.

XRD Analysis of Synthesized Nanocarbon NC-10 from Rice Husk Char

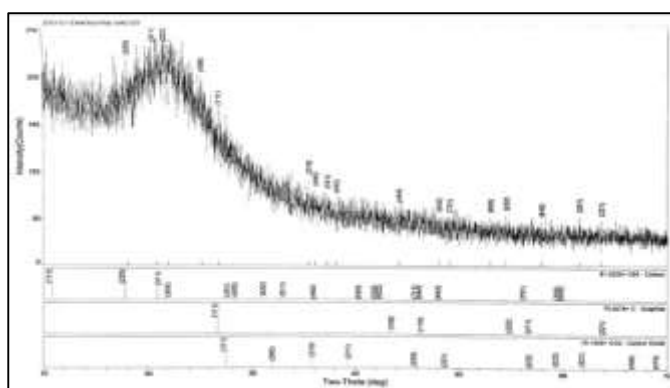


Figure 12 XRD diffraction pattern of nanocarbon NC-10 from rice husk char

The crystallite size and crystal structure of nanocarbon NC-10 from the rice husk char was determined from the XRD study.

Table 11 The average particle size of nanocarbon NC-10 from rice husk char

Peak No.	Bragg angle (2θ)	Miller indices (h k l)	FWHM of peak (β) radians	Particle size, D (nm)
1	17.952	(2 2 0)	0.0042	33.050
2	20.773	(3 1 1)	0.0088	15.840
3	21.858	(2 2 2)	0.0081	17.240
4	37.280	(5 3 1)	0.0109	13.275
5	38.154	(4 4 2)	0.0026	55.799
6	63.707	(2 2 1)	0.0019	84.958

The localized peaks at $2\theta = 17.952^\circ$, 20.773° , 21.858° , 37.280° , 38.154° and 63.707° that referred to plane reflections of (220), (311), (222), (531), (442) and (221), respectively. The broad peak at around 26° confirms the presence of amorphous nanocarbon material. According to Table 11, the range of particle size of synthesized nanocarbon NC-10 from rice husk char was found to be 13.275nm-84.958 nm and average particle size is 37.220 nm.

Table 12 The average crystalize sizes and lattice crystal nature for all nanocarbons

No	Nanocarbon	Average crystalize size	Lattice crystal nature
1	NC-1	44.2320	Hexagonal
2	NC-2	32.5489	Cubic
3	NC-3	34.7114	Cubic
4	NC-4	41.1630	Hexagonal
5	NC-5	42.2241	Cubic
6	NC-6	35.2175	Cubic
7	NC-7	31.8670	Hexagonal
8	NC-8	36.8098	Cubic
9	NC-9	44.1708	Cubic
10	NC-10	37.2200	Cubic

In this table, the lattice crystal natures of synthesized nanocarbons are cubic and hexagonal. According to the XRD patterns, the average crystalize sizes and lattice crystal nature for all nanocarbons are 32.5489 nm, 34.7114 nm, 41.1630 nm, 42.2241 nm, 35.2175 nm, 31.8670 nm, 36.8098 nm, 44.1708 nm and 37.2200 nm are respectively. Thus, all the data are in the range of nanoparticle scale 1 nm to 100 nm.

SEM Analysis

The morphologies of prepared nanocarbons are investigated by SEM microscopy. Figure 13 (a) and (b) shows the morphologies of nanocarbon NC-8 and nanocarbon NC-10.

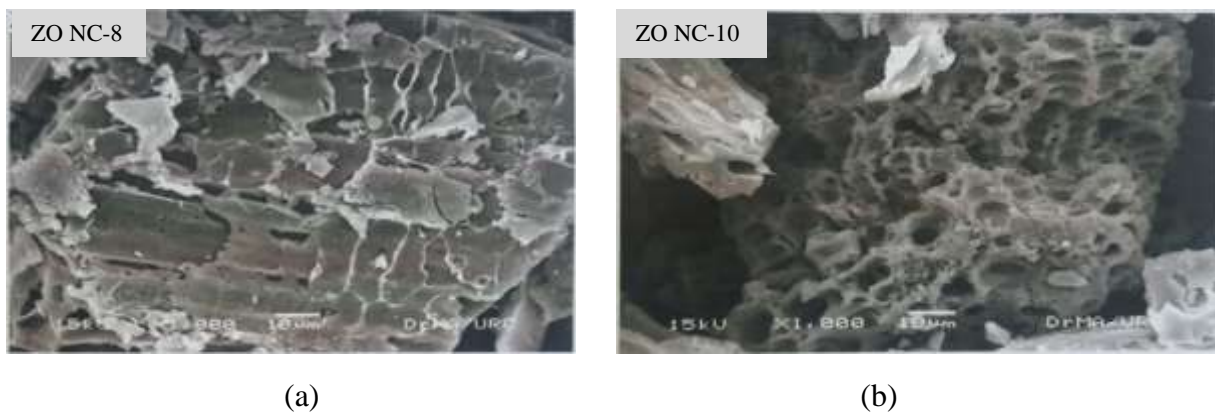


Figure 13 SEM micrographs of (a) nanocarbon NC-8 and (b) nanocarbon NC-10

The SEM micrographs suggest that the material has non regular compacted surface with cavities. This could be due to breakdown of the lignocellulosic material and evaporation of volatile compounds that leave the nanocarbons with well developed pores.

Conclusion

In this research work, the preparation of nanocarbons (NC-1 to NC-6) was carried out from rice husk char by NaNO_3 , KMnO_4 and H_2SO_4 by Modified Hummer Method with various conditions. Similarly, the preparation of nanocarbons (NC-7 to NC-11) was carried out from rice husk char by H_3PO_4 , KMnO_4 and H_2SO_4 with various conditions. Moreover, studying on the X-ray diffraction (XRD) analysis, the lattice crystal nature of the synthesized nanocarbon was observed as cubic and hexagonal. The average crystal sizes of synthesized nanocarbon are 44.232 nm, 32.549 nm, 34.711 nm, 47.163 nm, 42.224 nm, 35.218 nm, 31.867 nm, 36.8098 nm, 44.171 nm, 37.220 nm and 57.645 nm respectively. Finally, the morphology of the synthesized nanocarbon NC-8 and NC-10 are investigated by Scanning Electron Microscopy (SEM) micrograph indicate the non regular compacted surface with cavities and protuberances. Nanocarbons can be prepared from the waste rice husks for application in electrochemical energy storage, biogenetic and organic solar cells.

Acknowledgements

I would like to express my gratitude to Dr Yi Yi Myint, Professor and Head, Department of Chemistry, University of Mandalay, for her guidance to do this research work. I also thank to all of my teachers from whom I have learned and to all my friends for their patience and understanding during my research work.

References

- AOAC (2000). "Official Methods of Analysis". 17th Edition, The Association of Official Analytical Chemists, USA. Methods 925.10, 65.17, 974.24, 992.16.
- Ajayan, P. M., Ebbesen, T. W., Ichihashi, T., Iijima, S., Tanigaki, K., and Hiura, H. (1993). Opening Carbon Nanotubes with Oxygen and Implications for Filling. *Nature*, 362(6420), 522-525.
- Balasubramanian, K., Lee, E. J., Weitz, R. T., Burghard, M., & Kern, K. (2008). Carbon Nanotube Transistors—Chemical Functionalization and Device Characterization. *Physica Status Solid (a)*, 205(3), 633-646.
- Bolotin, K. I., Sikes, K. J., Jiang, Z., Klima, M., Fudenberg, G., Hone, J. E., and Stormer, H. L. (2008). Ultrahigh Electron Mobility in Suspended Graphene. *Solid State Communications*, 146(9-10), 351-355.
- Ganin, A. Y., Takabayashi, Y., Khimyak, Y. Z., Margadonna, S., Tamai, A., Rosseinsky, M. J., & Prassides, K. (2008). Bulk Superconductivity at 38 K in a Molecular System. *Nature Materials*, 7(5), 367-371.
- Geim, A. K. (2009). Graphene: Status and Prospects. *Science*, 324(5934), 1530-1534.
- Kim, J., Page, A. J., Irlle, S., and Morokuma, K. (2012). Dynamics of Local Chirality during SWCNT Growth: Armchair versus Zigzag Nanotubes. *Journal of the American Chemical Society*, 134(22), 9311-9319.
- Kroto, H. W., Heath, J. R., O'Brien, S. C., Curl, R. F., and Smalley, R. E. (1985). C₆₀: Buckminsterfullerene. *Nature*, 318 (6042), pp. 162-163.
- Kybert, N. J., Lerner, M. B., Yodh, J. S., Preti, G., and Johnson, A. C. (2013). Differentiation of Complex Vapor Mixtures using Versatile DNA-carbon Nanotube Chemical Sensor Arrays. *ACS Nano*, 7(3), 2800-2807.
- Miyato, Y. (2011). Basics of Carbon Nanotube and Its Applications. *Journal of MMIJ*, 127(2), 61-68.
- Novoselov, K. S., Geim, A. K., Morozov, S. V., Jiang, D., Zhang, Y., Dubonos, S. V., and Firsov, A. A. (2004). Electric Field Effect in Atomically Thin Carbon Films. *Science*, 306(5696), 666-669.
- Novoselov, K. S., Geim, A. K., Morozov, S. V., Jiang, D., Katsnelson, M. I., Grigorieva, and Firsov, A. A. (2005). Two-dimensional Gas of Massless Dirac Fermions in Graphene. *Nature*, 438(7065), 197-200.
- Omachi, H., Nakayama, T., Takahashi, E., Segawa, Y., & Itami, K. (2013). Initiation of Carbon Nanotube Growth by well-defined Carbon Nanorings. *Nature Chemistry*, 5(7), 572-576.
- Park, J., Kim, Y., Kim, G. T., and Ha, J. S. (2011). Facile Fabrication of SWCNT/SnO₂ Nanowire Heterojunction Devices on Flexible Polyimide substrate. *Advanced Functional Materials*, 21(21), 4159-4165.
- Pesin, D., and MacDonald, A. H. (2012). Spintronics and Pseudospintronics in Graphene and Topological Insulators. *Nature materials*, 11(5), 409-416.
- Tanigaki, K., Ebbesen, T. W., Saito, S., Mizuki, J., Tsai, J. S., Kubo, Y., and Kuroshima, S. (1991). Superconductivity at 33 K in CsxRbyC₆₀. *Nature*, 352(6332), 222-223.
- Zhang, Y., Tan, Y. W., Stormer, H. L., & Kim, P. (2005). Experimental observation of the quantum Hall effect and Berry's phase in graphene. *nature*, 438(7065), 201-204.